Acta Crystallographica Section F
Structural Biology and Crystallization Communications
ISSN 1744-3091

Purification, crystallization and preliminary crystallographic analysis of banyan peroxidase

Anurag Sharma,[a]‡ Gottfried J. Palm,[b]*‡ Moni Kumari,[a] Santosh Panjikar,[c]§ M. V. Jagannadham[a]* and Winfried Hinrichs[b]

[a]Molecular Biology Unit, Institute of Medical Sciences, Banaras Hindu University, Varanasi 221 005, India, [b]Institute for Biochemistry, University of Greifswald, Felix-Hausdorff-Strasse 4, 17489 Greifswald, Germany, and [c]EMBL Hamburg Outstation, c/o DESY, Notkestrasse 85, 22603 Hamburg, Germany

‡ These authors made equal contributions.
§ Current address: Australian Synchrotron, 800 Blackburn Road, Clayton, Victoria 3168, Australia.

Correspondence e-mail: palm@uni-greifswald.de, jvm@bhu.ac.in

Received 9 March 2012
Accepted 8 June 2012

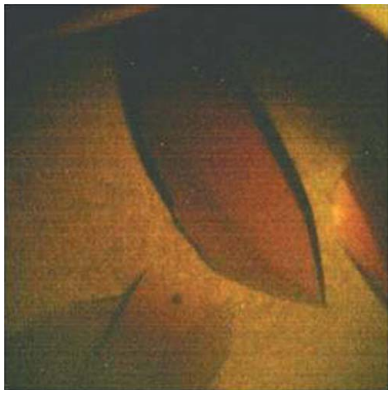

Plant peroxidases are extensively used in a wide range of biotechnological applications owing to their high environmental and thermal stability. A new peroxidase, named banyan peroxidase, was purified from the latex of *Ficus benghalensis* and crystallized. X-ray diffraction data were collected from native crystals and from bromide and xenon derivatives to resolutions of up to 1.66 Å in the trigonal space group $P3_221$, with unit-cell parameters $a = b = 73.1$, $c = 164.6$ Å. The anomalous signal of the intrinsic iron and calcium ions was sufficient for structure solution by SAD, although the sequence is not yet known.

1. Introduction

Enzymes that can tolerate extreme conditions of pH and temperature are widely used in biotechnological applications, particularly for biocatalysis. Peroxidases are known to be environmentally stable enzymes, especially those derived from thermophilic microorganisms (Rabe *et al.*, 2008) and higher plants (Rani & Abraham, 2006). Peroxidases are involved in several physiological processes in plants, including lignification and cell-wall formation (Wallace & Fry, 1999), protection against pathogens and wound healing (McLusky *et al.*, 1999), and abiotic and biotic stress responses (Avsian-Kretchmer *et al.*, 2004). They are heme-containing oxidoreductases that make use of hydrogen peroxide to oxidize various organic and inorganic substrates. Plant peroxidases have been divided into three classes (Welinder *et al.*, 1992): intracellular peroxidases (class I), extracellular fungal peroxidases (class II) and secretory plant peroxidases (class III). We describe a peroxidase from the latex of the banyan tree (*Ficus benghalensis*). Based on its source it is assigned to the class III peroxidases, which typically have an N-terminal polypeptide signal, two conserved calcium ions and four disulfide bridges. These enzymes have a conserved arginine and two histidine residues adjacent to the heme and extra helices that play an important role in the accessibility of the substrate to the heme. They are also glycoenzymes that bear up to eight asparagine-linked glycans which may contribute to protein stabilization (Welinder *et al.*, 1992). X-ray structures of class III plant peroxidases have been elucidated from horseradish (Gajhede *et al.*, 1997), peanut (Schuller *et al.*, 1996) and soybean (Henriksen *et al.*, 1998). Here, we describe the isolation, purification, crystallization and preliminary X-ray diffraction analysis of banyan peroxidase.

2. Experimental methods

2.1. Purification of banyan peroxidase

The stem of *F. benghalensis* was incised and fresh latex was collected in 10 m*M* Tris–HCl pH 7.5 and cooled to 253 K for 48 h. Subsequently, the latex was thawed to room temperature and centrifuged at 12 000*g* for 40 min to remove gum and other debris.

The crude latex extract was subjected to anion-exchange chromatography on DEAE-Sepharose Fast Flow (Sigma–Aldrich Chemie, Steinheim, Germany) in a column pre-equilibrated with 20 m*M* Tris pH 7.5. Bound proteins were eluted with a linear gradient from 0 to 0.4 *M* NaCl. All fractions were monitored for protein content by

Table 1
Purification of banyan peroxidase.

Step	Total protein (mg)	Total activity (units†)	Yield (%)	RZ ratio (A_{403}/A_{280})
Crude latex	5002	20100	100	0.3
DEAE-Sepharose	400	16020	80	2.1
Superdex 200	100	12000	60	3.2

† One unit of enzyme is defined as the amount of enzyme that catalyzes the formation of 1.0 µmol of product per minute under standard assay conditions. Pyrogallol was used as the substrate for activity measurements.

absorbance at 280 nm and were assayed for enzymatic activity using hydrogen peroxide as a first substrate and pyrogallol as a second substrate (Patel *et al.*, 2008). The homogeneity of the enzyme in all of the fractions was assessed by SDS–PAGE.

The protein fractions were pooled and dialyzed against 20 m*M* Tris–HCl pH 8.0 and concentrated using an ultrafiltration device (Vivaspin concentrator, 10 000 Da molecular-weight cutoff; Sartorius, Göttingen, Germany). The concentrated sample was subjected to gel filtration on a Superdex 200 16/60 column (GE Healthcare, Freiburg, Germany) pre-equilibrated and eluted with 0.2 *M* NaCl in 20 m*M* Tris–HCl pH 7.5 at a flow rate of 0.25 ml min^{-1}. 1 ml fractions were collected and assayed for protein content and peroxidase activity. The fractions with peroxidase activity were pooled, concentrated, desalted by ultrafiltration and further analyzed on SDS–PAGE for purity and homogeneity. The progress of purification is documented in Table 1. The obtained protein was pure and homogeneous and was stored at 273 K for further use.

2.2. Crystallization

The banyan peroxidase was screened for initial crystallization conditions by the sitting-drop vapor-diffusion method using a crystallization robot (HTPC; CyBio, Jena, Germany), 96-well plates (CrystalQuick Lp; Greiner Bio-One, Frickenhausen, Germany) and sparse-matrix screens (Hampton Research, Aliso Viejo, California, USA and Jena Bioscience, Jena, Germany). Initial hits were optimized in 24-well crystallization plates (Greiner Bio-One) using the hanging-drop vapor-diffusion method. Each well contained 500 µl reservoir solution. After optimization, crystals of native banyan peroxidase (30 mg ml^{-1} protein in 20 m*M* Tris–HCl pH 8.0) were obtained using a reservoir solution consisting of 1.3 *M* ammonium sulfate and 1.0 *M* lithium sulfate. For the hanging drops, 1 µl native protein solution was mixed with 1 µl reservoir solution. The pH after mixing was not measured. Crystallization trays and solutions were kept on ice during setup of the crystallization plates but were stored at 293 K (Bogdanović & Hinrichs, 2011).

2.3. Bromide soaking and xenon derivatization

A bromide derivative was prepared by soaking crystals in 1 *M* NaBr and 20% glycerol in reservoir solution for 10 s and flash-cooling in liquid nitrogen (Panjikar & Tucker, 2002*a*). A xenon derivative was prepared by transferring the crystals to well solution prepared with 20% glycerol. The crystal was then transferred to a pressure cell (Hampton Research) and pressurized under a 4 MPa xenon atmosphere for 1 min (Panjikar & Tucker, 2002*b*,*c*). The pressure was released slowly over 30 s and the crystal was immediately flash-cooled in liquid nitrogen.

2.4. Data collection and processing

Diffraction data were collected from single crystals on the EMBL beamlines at the DESY synchrotron source, Hamburg, Germany. The crystals were soaked in a cryoprotectant consisting of 15%(*v*/*v*) glycerol in reservoir solution and flash-cooled to 100 K. A native data set was collected to a resolution of 1.8 Å on beamline X11 equipped with a MAR 555 detector (MAR Research, Norderstedt, Germany). An anomalous data set was collected from a native crystal at a longer wavelength (1.4586 Å) on beamline X12 using a MAR CCD 225 detector, assuming the presence of Fe in the heme cofactor. A MAD data set was collected from a bromide-soaked crystal at the Br *K* absorption edge. Data were collected from a xenon-pressurized crystal on beamline X12 as a long-wavelength data set for maximal anomalous signal and at a short wavelength for high resolution.

All data were processed with *MOSFLM* (Leslie & Powell, 2007) and scaled using *SCALA* from the *CCP*4 suite (Winn *et al.*, 2011) (data collected on beamline X11) or processed with *XDS* (Kabsch, 2010). Structure-factor amplitudes were obtained from intensities

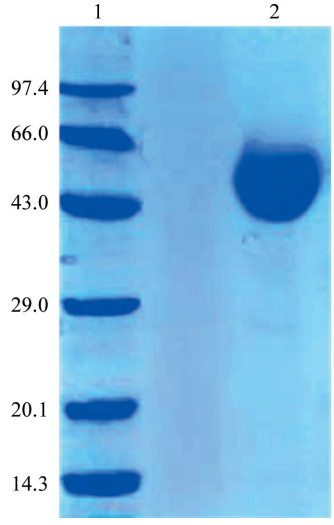

Figure 1
Assessment of the homogeneity and the molecular weight of the enzyme by 15% SDS–PAGE. Lanes 1 and 2 contain molecular-weight marker (labelled in kDa) and purified banyan peroxidase, respectively.

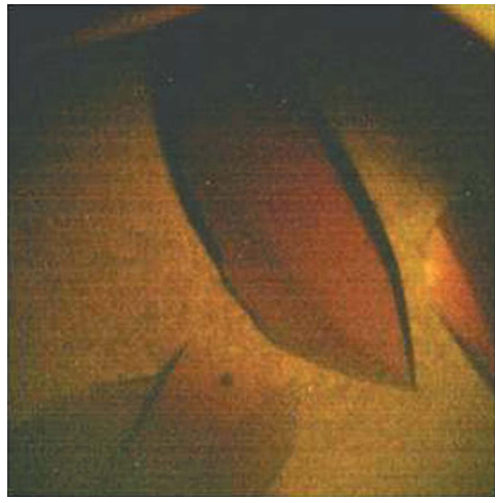

Figure 2
Crystals of native banyan peroxidase from *F. benghalensis* in dark brown drops.

Table 2
Data-collection and processing statistics.

Values in parentheses are for the highest resolution shell. Friedel pairs were not merged except for the native data set collected on beamline X11.

			Bromide soak†				
	Native		Peak	Infl	Hrem	Xenon pressurized	
Beamline (EMBL at DESY)	X11	X12	X12			X12	
Wavelength (Å)	0.81738	1.4586	0.91973	0.92007	0.9183	1.44163	1.00000
Space group	$P3_221$	$P3_221$	$P3_221$	$P3_221$	$P3_221$	$P3_221$	$P3_221$
Unit-cell parameters (Å)							
a	72.2	72.1	72.9	72.7	72.3	73.0	73.1
c	164.9	164.7	165.1	165.0	164.8	164.5	164.6
Resolution (Å)	1.80 (1.90–1.80)	2.90 (3.07–2.90)	2.60 (2.75–2.60)	2.60 (2.76–2.60)	2.31 (2.44–2.31)	2.20 (2.33–2.20)	1.66 (1.76–1.66)
No. of unique reflections	46677 (6789)‡	21144 (3278)	30067 (4675)	29928 (4635)	42183 (6544)	49356 (7801)	114759 (18133)
Multiplicity	4.2 (4.3)	8.0 (7.7)	11.6 (11.3)	11.6 (11.4)	3.9 (3.8)	3.9 (3.8)	7.4 (6.9)
Completeness (%)	99.3 (100.0)	99.3 (98.1)	99.4 (97.8)	99.3 (96.7)	99.2 (96.6)	99.4 (98.3)	99.6 (97.7)
$R_{\rm merge}$§	0.071 (0.525)	0.090 (0.396)	0.074 (0.436)	0.078 (0.474)	0.071 (0.494)	0.034 (0.152)	0.046 (0.990)
$\langle I/\sigma(I)\rangle$	8.4 (1.8)	22.8 (6.2)	27.4 (5.5)	26.4 (5.2)	14.1 (2.2)	26.1 (8.4)	22.9 (2.4)
$\mathrm{Corr}_{\rm anomalous}$ [resolution¶]	−0.245 [−]	0.14 [3.8 Å]	0.16 [3.6 Å]	0.16 [3.6 Å]	0.10 [3.5 Å]	0.25 [2.3 Å]	0.07 [2.5 Å]

† Wavelengths for data collection from the bromide-soaked crystal were chosen to be at the peak, inflection point (infl) and high-energy remote (hrem) of the Br *K* absorption edge. ‡ Friedel pairs merged. § $R_{\rm merge} = \sum_{hkl}\sum_i |I_i(hkl) - \langle I(hkl)\rangle| / \sum_{hkl}\sum_i I_i(hkl)$, where $I_i(hkl)$ is the observed intensity of an individual reflection and $\langle I(hkl)\rangle$ is the average intensity of that reflection. ¶ Highest resolution at which the anomalous correlation is greater than 0.10, *i.e.* useful.

with *TRUNCATE* (French & Wilson, 1978; Winn *et al.*, 2011). Statistics of the processed and scaled data are given in Table 2.

2.5. Structure solution

Initial phasing was attempted at the beamline using the *Auto-Rickshaw* protocol (Panjikar *et al.*, 2005, 2009), which incorporates various *CCP*4 programs, including *CAD* and *SCALEIT* (Winn *et al.*, 2011), *SHELXC*/*D*/*E* (Sheldrick, 2008), *SHARP* (Bricogne *et al.*, 2003), *BP*3 (Pannu & Read, 2004), *DM* (Cowtan, 1994), *RESOLVE* (Terwilliger, 2000) and *ARP*/*wARP* (Perrakis *et al.*, 1999).

3. Results and discussion

A new enzyme, banyan peroxidase, was purified from the latex of *F. benghalensis* (Table 1). The purity of the enzyme can be judged by the Reinheitszahl (RZ) value: the absorbance ratio A_{403}/A_{280}. The RZ value for the pure enzyme was 3.2, which is in good agreement with reported values of 2.5–3.5 for plant peroxidases. The molecular weight of banyan peroxidase was judged by SDS–PAGE, which showed a major single migration band at around 47 kDa (Fig. 1) demonstrating high purity. The diffuse protein band on SDS–PAGE may arise from variable glycosylation of the protein.

Several crystallization hits were found, but only reservoir solutions containing ammonium sulfate gave diffracting crystals. Small crystal plates which diffracted X-rays grew from 1.6 *M* ammonium sulfate, 1 *M* lithium sulfate (condition B3 of JBScreen Classic 6 from Jena Bioscience). Further optimization led to the production of lentil-shaped reddish crystals using 1.3 *M* ammonium sulfate, 1.0 *M* lithium sulfate. Crystals appeared within one week of crystallization setup and reached maximum dimensions of approximately 0.8 × 0.5 × 0.1 mm. These crystals of banyan peroxidase (Fig. 2) were suitable for X-ray data collection. An initial complete native data set was collected to a resolution of 1.8 Å. The unit-cell parameters indicated only one monomer per asymmetric unit ($V_{\rm M}$ = 2.6 Å^3 Da^{-1} for a 47 kDa monomer; Matthews, 1968) in the trigonal Laue class $\bar{3}m1$. The polypeptide sequence was not known at this point. The choice of a suitable molecular-replacement model was therefore not obvious. Using the tentative protein sequence obtained after structure solution, we were able to find structures that would have solved the data set using molecular replacement. The position of the expected iron could be located in the anomalous Patterson map or from the native data set collected at longer wavelength by using direct methods. However, the data quality was not sufficient to phase the whole structure. Bromide MAD phasing was also not successful. This is perhaps a consequence of the limited quality and resolution of the data, despite the fact that the data showed some anomalous signal (Table 2).

The xenon-pressurized crystal provided the best diffraction data. Its long-wavelength data revealed three heavy-atom positions, which turned out to be iron and two calcium ions, not xenon. The SAD phasing protocol of *Auto-Rickshaw* provided a partial model with 291 residues in space group $P3_221$. A preliminary inspection of the map showed additional electron density for the heme group (Fig. 3). Crystallographic refinement and assignment of the protein sequence using the high-resolution data is currently in progress.

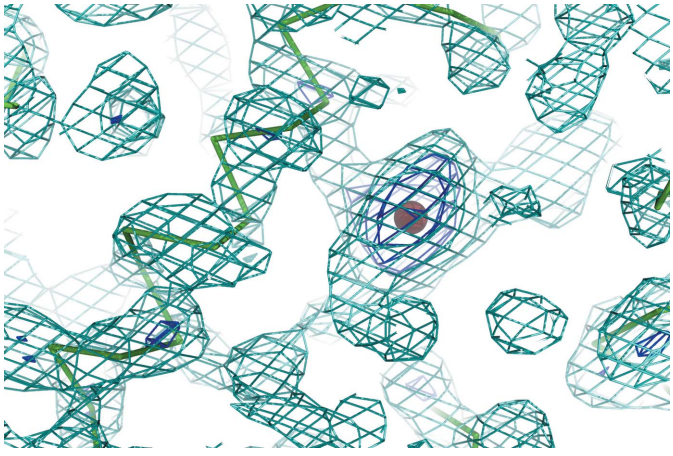

Figure 3
Experimental electron-density map after density modification at 1.5σ (light blue) and 5σ (dark blue). To the left of the iron position (brown sphere) of the presumed heme an α-helix is visible as part of the modelled C$^\alpha$ trace.

Financial assistance to AS and MK in the form of a research fellowship from CSIR (Council of Scientific and Industrial Research), Government of India is gratefully acknowledged. Funding assistance to AS from the Boehringer Ingelheim Fonds, Germany and the

Robert Bosch Stiftung, Germany for establishing collaboration in Germany is gratefully acknowledged.

References

Avsian-Kretchmer, O., Gueta-Dahan, Y., Lev-Yadun, S., Gollop, R. & Ben-Hayyim, G. (2004). *Plant Physiol.* **135**, 1685–1696.

Bogdanović, X. & Hinrichs, W. (2011). *Acta Cryst.* F**67**, 421–423.

Bricogne, G., Vonrhein, C., Flensburg, C., Schiltz, M. & Paciorek, W. (2003). *Acta Cryst.* D**59**, 2023–2030.

Cowtan, K. (1994). *Jnt CCP4/ESF–EACBM Newsl. Protein Crystallogr.* **31**, 34–38.

French, S. & Wilson, K. (1978). *Acta Cryst.* A**34**, 517–525.

Gajhede, M., Schuller, D. J., Henriksen, A., Smith, A. T. & Poulos, T. L. (1997). *Nature Struct. Biol.* **4**, 1032–1038.

Henriksen, A., Welinder, K. G. & Gajhede, M. (1998). *J. Biol. Chem.* **273**, 2241–2248.

Kabsch, W. (2010). *Acta Cryst.* D**66**, 125–132.

Leslie, A. G. W. & Powell, H. R. (2007). *Evolving Methods for Macromolecular Crystallography*, edited by R. J. Read & J. L. Sussman, pp. 41–51. Dordrecht: Springer.

Matthews, B. W. (1968). *J. Mol. Biol.* **33**, 491–497.

McLusky, S. R., Bennett, M. H., Beale, M. H., Lewis, M. J., Gaskin, P. & Mansfield, J. W. (1999). *Plant J.* **17**, 523–534.

Panjikar, S., Parthasarathy, V., Lamzin, V. S., Weiss, M. S. & Tucker, P. A. (2005). *Acta Cryst.* D**61**, 449–457.

Panjikar, S., Parthasarathy, V., Lamzin, V. S., Weiss, M. S. & Tucker, P. A. (2009). *Acta Cryst.* D**65**, 1089–1097.

Panjikar, S. & Tucker, P. A. (2002*a*). *Acta Cryst.* D**58**, 1413–1420.

Panjikar, S. & Tucker, P. A. (2002*b*). *J. Appl. Cryst.* **35**, 261–266.

Panjikar, S. & Tucker, P. A. (2002*c*). *J. Appl. Cryst.* **35**, 117–119.

Pannu, N. S. & Read, R. J. (2004). *Acta Cryst.* D**60**, 22–27.

Patel, A. K., Singh, V. K., Moir, A. J. & Jagannadham, M. V. (2008). *J. Agric. Food Chem.* **56**, 9236–9245.

Perrakis, A., Morris, R. & Lamzin, V. S. (1999). *Nature Struct. Biol.* **6**, 458–463.

Rabe, K. S., Kiko, K. & Niemeyer, C. M. (2008). *Chembiochem*, **9**, 420–425.

Rani, D. N. & Abraham, T. E. (2006). *Appl. Biochem. Biotechnol.* **128**, 215–226.

Schuller, D. J., Ban, N., Huystee, R. B., McPherson, A. & Poulos, T. L. (1996). *Structure*, **4**, 311–321.

Sheldrick, G. M. (2008). *Acta Cryst.* A**64**, 112–122.

Terwilliger, T. C. (2000). *Acta Cryst.* D**56**, 965–972.

Wallace, G. & Fry, S. C. (1999). *Phytochemistry*, **52**, 769–773.

Welinder, K. G., Mauro, J. M. & Nørskov-Lauritsen, L. (1992). *Biochem. Soc. Trans.* **20**, 337–340.

Winn, M. D. *et al.* (2011). *Acta Cryst.* D**67**, 235–242.